the long-day–dependent and –independent pathways of floral induction (*1*, *7*, *8*, *11*). Indeed, in contrast to plants that overexpressed only *FT* or *LFY* (*12*), the vegetative phase was bypassed in *35S::FT 35S::LFY* plants, which produced a terminal flower immediately upon germination. The only leaves produced by these plants were the first two leaves, which are already initiated in the embryo (Fig. 2, C, E, and I, and Table 1). A less marked effect was seen in *35S::FT 35S::API* plants (Fig. 2C and Table 1), even though *35S::API* plants on their own flowered considerably earlier than did *35S::LFY* plants (*7*, *12–14*) (Table 1). The *35S::FT 35S::LFY* phenotype was also more severe than that of *35S::API 35S::LFY* plants (*14*), indicating that *FT* does not only induce *API*, which is confirmed by a failure of an *ap1* mutation to suppress early flowering of *35S::FT* plants (Table 1).

The deduced FT protein belongs to a small family of *Arabidopsis* proteins, which includes the TFL1 protein, whose amino acid sequence is more than 50% identical to that of FT (*3*, *15*). *FT* and *TFL1* have opposite effects on flowering. Loss of *FT* function causes late flowering (*4*), whereas loss of *TFL1* causes early flowering along with the formation of terminal flowers (*16*). However, *FT* and *TFL1* effects are not entirely mirror images of each other, because *35S::FT* plants flower much earlier than *tfl1* loss-of-function mutants, particularly under short days, and *35S::TFL1* plants not only flower late, as do *ft* loss-of-function mutants, but they also show transformation of individual flowers into shootlike structures (*17*).

To clarify the relation between *FT* and *TFL1*, we tested whether *FT* promotes flowering by eliminating *TFL1* activity. *35S::FT tfl1-1* plants flowered even earlier than *35S::FT* plants and often formed only a single, terminal flower on the main shoot, indicating that *TFL1* is still active in *35S::FT* (Table 1 and Fig. 2, A and H). Consistent with this finding, *TFL1* was expressed in *35S::FT* plants (Fig. 3, C and F). Independent action of *FT* and *TFL1* was likewise evident from the fact that *35S::TFL1* attenuated the early flowering of *35S::FT*, even though the attenuation was modest (Table 1 and Fig. 2A). Together, these observations suggest that *FT* and *TFL1* act at least partially in parallel.

TFL1 mRNA is highly expressed in a small group of shoot meristem cells (*15*) (Fig. 3F). Using reverse transcriptase polymerase chain reaction (RT-PCR), we detected *FT* mRNA throughout the aerial part of the plant (Fig. 1B). In situ hybridization revealed no specific concentration of *FT* transcripts at the shoot apex, suggesting that *FT* and *TFL1* do not have to be expressed in the same pattern to antagonize each other's effects.

FT and TFL1 are related to a membrane-associated mammalian protein that can bind hydrophobic ligands (*18*). This protein also gives rise to hippocampal cholinergic neurostimulating peptide (HNCP), which is generated from its precursor by cleavage after amino acid 12 (*19*). Comparison of the FT and TFL1 sequences (*3*) with the crystal structure (*20*, *21*) of HCNP precursor, also called phosphatidylethanolamine binding protein (PEBP), revealed several interesting features. The conserved residue Arg^{119} has been proposed to activate the bond between Leu^{12} and Ser^{13} for cleavage of HCNP (*20*). Arg^{119} is important for FT function as well, because this residue was changed to histidine in the strong *ft-3* allele (Fig. 1A). It has also been proposed that access to the PEBP ligand-binding site is regulated by a COOH-terminal α helix (*20*, *21*). A missense mutation in *ft-1* close to the COOH-terminus indicates that this region is critical for FT as well (Fig. 1A).

In summary, *FT* and *TFL1* encode related proteins with opposite effects on flowering. Similarly to *FT*, its antagonist *TFL1* is positively regulated by *CO* (*6*), suggesting that the balance between *FT* and *TFL1* activity serves to fine tune the response to floral inductive signals (*3*). It remains to be determined how far the sequence similarity between FT, TFL1, and mammalian PEBP reflects similar biochemical modes of action.

Note added in proof: Human PEBP was recently shown to be identical to RKIP (Raf kinase inhibitor protein), which regulates the activity of the RAF/MEK/ERK signal transduction pathway (*22*).

References and Notes

1. Y. Y. Levy and C. Dean, *Plant Cell* **10**, 1973 (1998).
2. H. Hayashi *et al.*, *Science* **258**, 1350 (1992).
3. See supplementary material at www.sciencemag.org/feature/data/1044618.shl. GenBank accession number for *FT* is AF152096.
4. M. Koornneef, C. J. Hanhart, J. H. van der Veen, *Mol. Gen. Genet.* **229**, 57 (1991).
5. M. Koornneef *et al.*, *Genetics* **148**, 885 (1998).
6. R. Simon, M. I. Igeño, G. Coupland, *Nature* **382**, 59 (1996).
7. O. Nilsson *et al.*, *Genetics* **150**, 403 (1998).
8. L. Ruiz-García *et al.*, *Plant Cell* **9**, 1921 (1997).
9. J. Putterill *et al.*, *Cell* **80**, 847 (1995).
10. F. Parcy *et al.*, *Nature* **395**, 561 (1998); D. Wagner *et al.*, *Science* **285**, 582 (1999).
11. M. A. Blázquez, L. Soowal, I. Lee, D. Weigel, *Development* **124**, 3835 (1997).
12. D. Weigel and O. Nilsson, *Nature* **377**, 495 (1995).
13. M. A. Mandel and M. F. Yanofsky, *Nature* **377**, 522 (1995).
14. S. J. Liljegren *et al.*, *Plant Cell* **11**, 1007 (1999).
15. D. Bradley *et al.*, *Science* **275**, 80 (1997).
16. S. Shannon and D. R. Meeks-Wagner, *Plant Cell* **3**, 877 (1991); J. Alvarez, C. L. Guli, X.-H. Yu, D. R. Smyth, *Plant J.* **2**, 103 (1992).
17. O. Ratcliffe *et al.*, *Development* **125**, 1609 (1998).
18. F. Schoentgen, F. Saccoccio, J. Jolles, I. Bernier, P. Jolles, *Eur. J. Biochem.* **166**, 333 (1987); D. K. Grandy *et al.*, *Mol. Endocrinol.* **4**, 1370 (1990).
19. N. Tohdoh, S. Tojo, H. Agui, K. Ojika, *Brain Res. Mol. Brain. Res.* **30**, 381 (1995).
20. M. J. Banfield *et al.*, *Structure* **6**, 1245 (1998).
21. L. Serre *et al.*, *Structure* **6**, 1255 (1998).
22. K. Yeung *et al.*, *Nature* **401**, 173 (1999).
23. F. D. Hempel *et al.*, *Development* **124**, 3845 (1997).
24. O. J. Ratcliffe, D. J. Bradley, E. S. Coen, *Development* **126**, 1109 (1999).

25. Special thanks to T. Araki for exchanging information on *FT* and the gift of *ft* deletion mutants. We thank C. Graham, S. Haaksma, V. Hedquist, H. Trinh, and D. Wolfe for assistance; M. Koornneef for unpublished information; our colleagues at the Salk Institute and G. Coupland, O. Nilsson, O. Ratcliffe, and M. Yanofsky for discussion; and G. Coupland, I. Igeño, M. Koornneef, S. Liljegren, and the NSF-supported ABRC for material. Supported by the Samuel Roberts Noble Foundation (I.K. and M.J.H.), KOSEF and the Hoffman Foundation (J.H.A.), the Howard Hughes Medical Institute (J.C.), and the NSF (S.K.C. and D.W.).

17 August 1999; accepted 7 October 1999

Organogenic Role of B Lymphocytes in Mucosal Immunity

Tatyana V. Golovkina,[1] Mark Shlomchik,[2,3] Lynn Hannum,[2] Alexander Chervonsky[1]*

Follicle-associated epithelium (FAE) in the intestinal Peyer's patches contains M cells that deliver pathogens to organized lymphoid tissue. Development of Peyer's patches, FAE, and M cells was found to be impaired in mice that had no B cells. Transgenic expression of membrane-bound immunoglobulin M restored B cells and FAE development. The lack of M cells abrogated infection with a milk-borne retrovirus. Thus, in addition to secretion of antibodies and presentation of antigens, B cells are important for organogenesis of the mucosal immune barriers.

The gut-associated lymphoid tissue (GALT) consists of highly organized Peyer's patches (PPs) in the small intestine and intraepithelial lymphocytes (IELs) found throughout the length of the gastrointestinal tract. The intestinal surface of PPs is characterized by the presence of FAE-covering "domes," regions free of intestinal villi (*1*). M cells are found in these domes, scattered among enterocytes (*2*). M cells lack microvilli on their apical

surface (hence the term M, denoting microfold or membranous cells) and are able to tunnel pathogens through the cytoplasm to the basal surface, where deep invaginations of their membrane allow close contact with lymphocytes and macrophages (*3*). In respiratory epithelium, where M cells are also found, they serve as the entrance gates for pathogens such as mycobacteria (*4*). In vitro, M cells were shown to develop from a human intestinal epithelial cell line under the influence of lymphocytes, and a B cell lymphoma was a stronger converter of epithelial cells into M cells than was a T cell lymphoma (*5*). Thus, we investigated whether B cells are responsible for the generation of FAE and M cells in vivo and whether B cell deficiency could affect transepithelial transport of an enterally transmitted retroviral pathogen.

We examined knockout (KO) mice with targeted mutations that lack specific lymphocyte subsets (*6*) for abnormalities in PP and FAE generation. The absence of B cells, due to KO of either the μ membrane segment (Igh-6) or J_H segments of immunoglobulin (Ig) genes (J_HD), caused a diminution of numbers of detectable PPs (Table 1). In contrast, mice deficient in either αβ T cells [T cell receptor (TCR)β KO] or γδ T cells (TCRδ KO) had normal numbers of PPs, as did mice deficient in both αβ and γδ T cells (TCRβ, TCRδ KO). The strongest PP deficiency has been observed in mice lacking both B and T cells as a result of the absence of RAG1 recombinase (RAG1 KO). In B cell–negative mice, the size of PPs was much smaller and FAE was abnormal, as revealed in unfixed preparations of PPs seen in transmitted light (Fig. 1, C and D) or in a cryostat section (Fig. 1G). The transgenic expression of a membrane-bound immunoglobulin M (mIgM) on the J_HD background, allowing generation of B cells with surface but not secreted IgM, completely restored the development of PPs (Table 1) and FAE (Fig. 1, E, F, and H).

Scanning electron microscopy (SEM) was used for further analysis of FAE in mutant mice (Fig. 2). SEM is the most adequate approach for M cell detection, as the luminal surface of M cells has very distinct microfold morphology (Fig. 2C) (*7*). SEM allows analysis of the large FAE surfaces, an advantage over transmission electron microscopy or histochemical detection of M cells (*8*). M cells could be found in abundance in the large domes in the PPs of normal mice (Fig. 2B) (*9*). In contrast, only a few cells with a characteristic microfold surface could be detected in the smaller domes of B cell–deficient animals (Fig. 2, E to G) (*9*). Cells with an unusual brush border (Fig. 2, F and G) were also found in mice without B cells. These cells are most likely M cell maturation intermediates (*9*).

Reconstitution of B cells by mIgM transgene expression resulted in the complete development of FAE and M cells (Fig. 2, H and I). Nonactivated B lymphocytes are likely sufficient for organogenesis, as FAE-containing M cells were normally developed in CD40 ligand–negative (CD40L KO) mice (Fig. 2J), even though B cells in these mice cannot be properly activated (*10, 11*). The lack of T cells did not have any significant influence on FAE development because TCRβ, TCRδ KO mice had normally developed M cells (Fig. 2K). However, in RAG1 KO mice, domes were even more difficult to find than in mice with no B cells, and there was no evidence of M cells (*12*); this suggests that the development of residual M cells found in the absence of B cells (Fig. 2, F and G) (*9*) may be promoted by T lymphocytes, although the input of T cells in M cell devel-

[1]Jackson Laboratory, 600 Main Street, Bar Harbor, ME 04609, USA. [2]Section of Immunobiology, [3]Department of Laboratory Medicine, Yale University School of Medicine, New Haven, CT 06510, USA.

*To whom correspondence should be addressed. E-mail: avc@aretha.jax.org

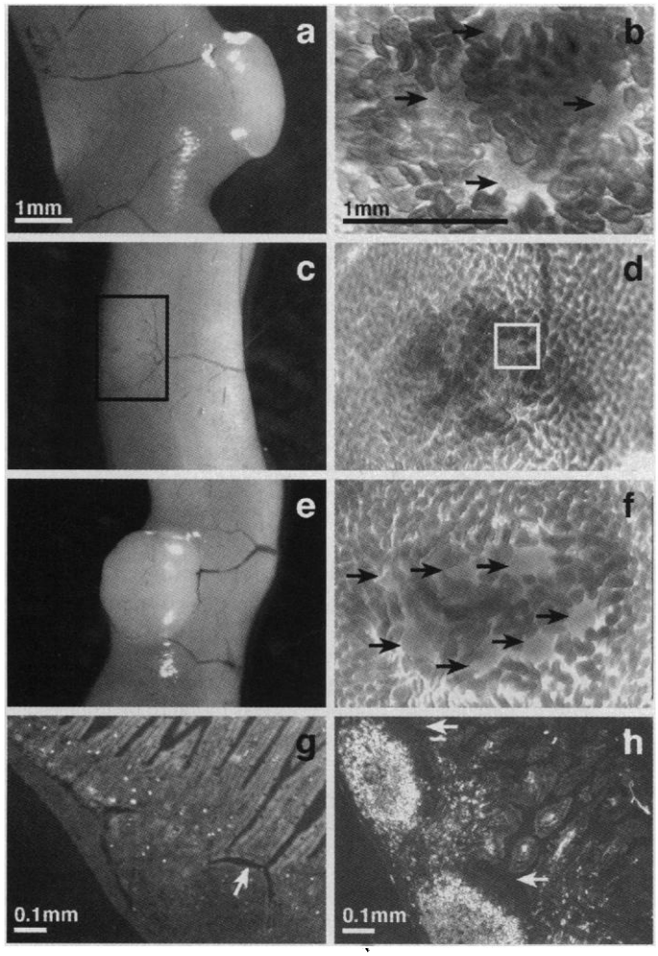

Fig. 1. Full development of PPs and FAE is affected in B cell–negative mice and can be restored by transgenic expression of mIgM. Relative to normal B6 mice (**A** and **B**), two B cell–deficient mouse stocks analyzed—Igh-6 (**C** and **D**) and J_HD (**G**)—showed reductions in PP size, dome numbers, and dome size. Transgenic expression of mIgM led to development of B cells (**H**), PPs, and domes (**E** and **F**). The inner surface of PPs was photographed in transmitted light using a Wild M10 Stereoscope (Leica) and SPOT charge-coupled device camera (Diagnostic Instruments, Sterling Heights, Michigan). Black rectangle, PP in Igh-6 mouse; black and white arrows, FAE; white rectangle, FAE in Igh-6 mouse. Scale bar for (A), (C), and (E) is shown in (A); bar for (B), (D), and (F) is shown in (B). Cryostat sections of PPs from J_HD (G) and transgenic mIgM (H) mice were stained with fluorescein isothiocyanate–coupled polyclonal antibodies to Ig (Sigma).

Table 1. Development of Peyer's patches is affected in mice lacking B lymphocytes.

Mouse strain	PP numbers	
	Average	Individual mice
B6	6.8	7, 5, 7, 6, 5, 9, 8, 7, 6, 8, 7
B6-Igh-6	2.1*	3, 2, 2, 2, 3, 2, 2, 3, 2, 1, 2, 2, 2, 2, 2
B6-TCRβ KO	7.0	7, 7, 6, 8, 7, 7
B6-TCRδ KO	6.3	5, 7, 6, 7
B6-TCRβ, TCRδ KO	6.8	6, 8, 7, 6, 7, 7
B6-Rag1 KO	0.6*	1, 0, 1, 0
BALB/cJ	10.3	11, 9, 10, 11
BALB/c-J_HD	1.6*	2, 0, 2, 0, 1, 2, 4, 2, 2, 1, 2
mIgM Tg	9.0	10, 11, 11, 8, 9, 10, 10, 7, 9, 10, 8, 8, 7

*The size of PPs was significantly diminished. PPs on isolated intestines were counted using a Leica MZ6 zoom stereo microscope (*28*).

opment is very limited. A conservative estimate suggests that the overall number of M cells in B cell–deficient mice is smaller by a factor of at least 150 to 840 (one-sixth to one-third the number of PPs × one-quarter to one-half the number of domes × one-fifth the dome surface area × one-seventh to one-fifth the number of M cells in the field). Thus, only 1.2 to 6.6 M cells are present in B cell–deficient mice per every 1000 M cells in normal intestine.

Substantial diminution of M cell numbers should lead to a strong functional impairment. We used mouse mammary tumor virus (MMTV), a classical retrovirus suspected to use M cells to enter GALT (*13*), to show functional involvement of M cells in retroviral transport from the intestinal lumen. MMTV infects only dividing cells, and it relies on its superantigen (SAg) to induce proliferation of T cells expressing certain Vβ chains (*14*). T cell activation by SAg depends on direct interaction with B lymphocytes (*15*). Elimination of either T cells with appropriate Vβ chains (*16*) or B cells (*17*) abrogates MMTV infection. Thus, B cells may be needed both for T cell activation and for M cell–dependent translocation of MMTV.

To unmask the possible role of M cells in channeling MMTV through the intestinal wall, we used a bone marrow (BM) chimera approach (*18*). Newborn Igh-6 or TCRβ KO mice were used as recipients of normal adult B6 BM and were simultaneously briefly exposed to MMTV (*19*). In all TCRβ KO (having intact B and M cells) recipients of B6 BM, MMTV infection was readily detectable (Fig. 3). In contrast, chimeras with a reconstituted immune system but with underdeveloped FAE were significantly resistant to MMTV infection: Most Igh-6 recipients had severely diminished viral load or had no detectable MMTV proviruses at all (Fig. 3). Only a small fraction of total T cells (T cells expressing cognate Vβ regions) can be used by MMTV (*20*). Nevertheless, T cell numbers originating from donor BM were sufficient to allow MMTV infection in B6 → TCRβ KO chimeras. Because mouse BM contains 15 to 20% cells of the B cell lineage versus 1 to 2% of the T cell lineage, the number of B cells introduced should be sufficient to support SAg-dependent T cell activation.

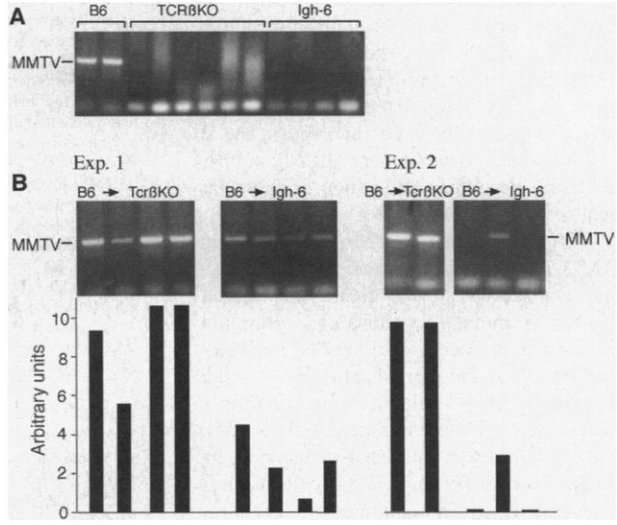

Fig. 3. Infection with milk-borne retrovirus (MMTV) is controlled by B cell–dependent FAE. (**A**) Control B6 mice, but not TCRβ KO or Igh-6 mice, fed with MMTV-laden milk became infected. Integrated MMTV proviruses were detected in the spleens at 8 weeks by semiquantitative PCR. Each lane represents a different mouse. (**B**) When the two immunodeficient strains were reconstituted at birth with B6 BM (*18*), only B6 → TCRβ KO chimeras demonstrated full-scale infection. Mice in the two experiments shown were fostered by MMTV$^+$ foster mothers for 7 and 3 days, respectively. Densitometric analysis of the PCR bands is shown below.

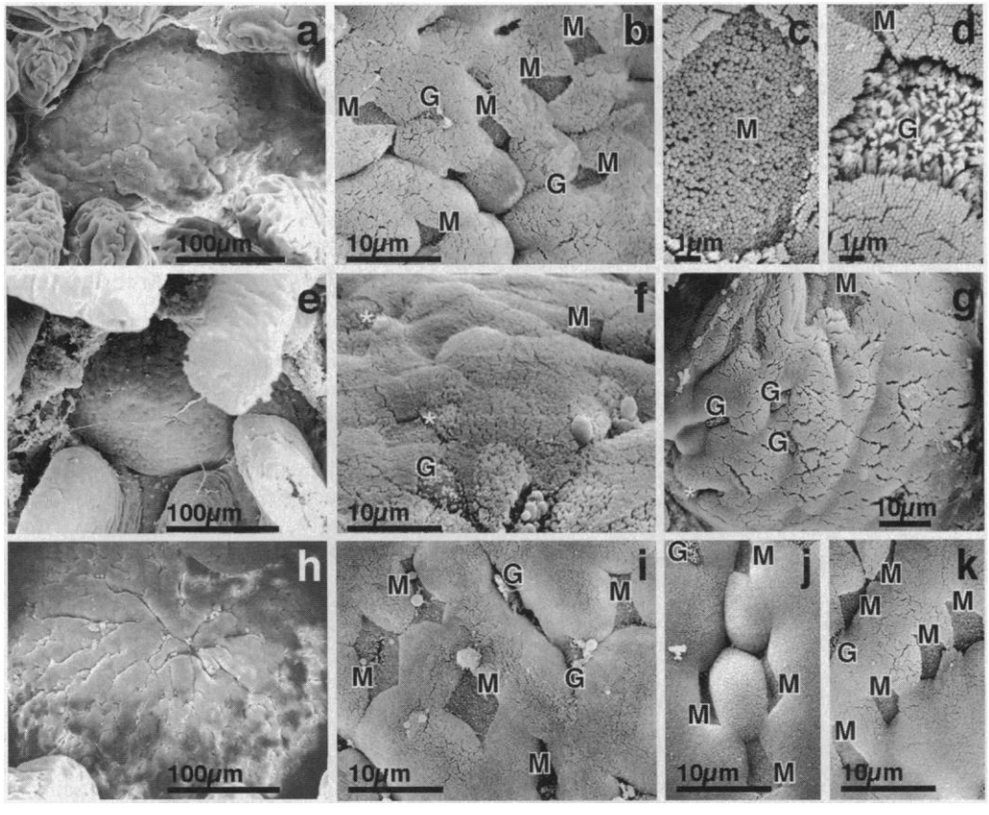

Fig. 2. SEM (*29*) showed normal FAE and the presence of M cells (marked "M") in BALB/cJ (**A** to **D**) and transgenic mIgM (**H** and **I**) mice. Goblet cells are indicated by "G"; enlarged images of a typical M cell (C) and goblet cell (D) are shown. In J_HD mice, FAE was small (**E** and **G**) and M cell generation (**F** and G) (*9*) was affected by the lack of B cells. Cells with an unusual brush border are marked with an asterisk in (F) and (G). (**J**) B cells in mice lacking CD40L stimulate normal development of FAE and M cells. (**K**) The absence of both αβ and γδ T cells did not affect M cell development.

The B cell–controlled development of FAE (as opposed to mere reduction of PP numbers) is crucial for retroviral infection, as tumor necrosis factor receptor 1 (TNFR1) KO mice with the same reduction in number and size of PPs (*21, 22*) as B cell–negative mice but with significant numbers of M cells were found to harbor MMTV efficiently (*9*).

The precise mechanisms of the organogenic function of B cells are unknown. B cells in transgenic mIgM mice do not produce any secreted Ig, excluding involvement of soluble Ig or signaling through Fc receptors in FAE development. The members of the TNFR family have been implicated in organogenesis of lymphoid tissue, including GALT (*23*), and are likely to be involved in the B cell–dependent development of FAE, similar to B cell–dependent generation of follicular dendritic cells (FDCs) (*24*).

The organogenic function of B cells in GALT (and possibly in other mucosal barriers, such as respiratory epithelium) is distinct from their immune functions of Ig secretion or antigen presentation. It affects M cell–dependent translocation of pathogens through mucosal barriers, influences an organism's interactions with environmental flora (*25*), and must be taken into account when interpreting studies that implicate B cells as antigen-presenting cells in immunity and autoimmunity (*26, 27*).

References and Notes

1. D. E. Bockman and M. D. Cooper, *Am. J. Anat.* **136**, 455 (1973).
2. R. L. Owen, *Gastroenterology* **72**, 440 (1977); M. R. Neutra, N. J. Mantis, A. Frey, P. J. Giannasca, *Semin. Immunol.* **11**, 171 (1999).
3. P. J. Sansonetti and A. Phalipon, *Semin. Immunol.* **11**, 193 (1999).
4. R. Teitelbaum *et al.*, *Immunity* **10**, 641 (1999).
5. S. Kernéis, A. Bogdanova, J.-P. Kraehenbuhl, E. Pringault, *Science* **277**, 949 (1997).
6. Mouse strains used and approved symbols: C57BL/6J (B6); BALB/cJ; B cell–deficient mice Igh-6 (C57BL/6J-Igh-6^{tm1Cgn}) [D. Kitamura, J. Roes, R. Kuhn, K. Rajewsky, *Nature* **350**, 423 (1991)]; J_HD (BALB/cJ-J_HD) [J. Chen *et al.*, *Int. Immunol.* **5**, 647 (1993)]; TC1Rβ KO (C57BL/6J-Tcrb^{tm1Mom}) and TCRβ, TCRδ KO (B6,129P-Tcrb^{tm1Mom} Tcrd^{tm1Mom}) [P. Mombaerts *et al.*, *Nature* **360**, 225 (1992)]; TCRδ KO (C57BL/6J-Tcrd^{tm1Mom}) [S. Itohara *et al.*, *Cell* **72**, 337 (1993)]; RAG1 KO (C57BL/6J-Rag1^{tm1Mom}) [P. Mombaerts *et al.*, *Cell* **68**, 869 (1992)]; TNFR1 KO (C57BL/ 6J-Tnfr1^{tm1Mak}) (*21*); CD40L KO (B6, 129S-Tnfsf5^{tm1Mom}) (*11*). Transgenic mIgM mice (BALB/cJ-IgM Tg) (*27*) were bred to BALB/cJ-J_HD mice for more than six generations at Yale University. All other animals were obtained from the Jackson Laboratory.
7. R. L. Owen, *Semin. Immunol.* **11**, 157 (1999).
8. M. A. Clark, M. A. Jepson, N. L. Simmons, T. A. Booth, B. H. Hirst, *J. Histochem. Cytochem.* **41**, 1679 (1993); R. L. Owen and D. K. Bhalla, *Am. J. Anat.* **168**, 199 (1983).
9. Supplemental information is available at *Science* Online (www.sciencemag.org/feature/data/1043897.shl).
10. R. J. Noelle *et al.*, *Proc. Natl. Acad. Sci. U.S.A.* **89**, 6550 (1992); E. A. Ranheim and T. J. Kipps, *J. Exp. Med.* **177**, 925 (1993).
11. B. R. Renshaw *et al.*, *J. Exp. Med.* **180**, 1889 (1994).
12. A. Chervonsky, data not shown.
13. O. Karapetian, A. N. Shakhov, J. P. Kraehenbuhl, H. Acha Orbea, *J. Exp. Med.* **180**, 1511 (1994). MMTV has also been introduced into adult mice by intranasal application [D. Velin, G. Fotopoulos, F. Luthi, J. P. Kraehenbuhl, *J. Exp. Med.* **185**, 1871 (1997)], suggesting that respiratory epithelium rich in M cells can serve as a gateway for the virus.
14. Y. Choi, J. W. Kappler, P. Marrack, *Nature* **350**, 203 (1991).
15. A. V. Chervonsky *et al.*, *Immunity* **3**, 139 (1995).
16. T. V. Golovkina, A. V. Chervonsky, J. P. Dudley, S. R. Ross, *Cell* **69**, 637 (1992); W. Held *et al.*, *Cell* **74**, 529 (1993).
17. U. Beutner, E. Kraus, D. Kitamura, K. Rajewsky, B. T. B. Huber, *J. Exp. Med.* **179**, 1457 (1994).
18. Newborn mice were irradiated with 200 rad, inoculated intravenously with 10^5 B6 BM cells the same day, reinoculated intraperitoneally with the same dose of BM for two additional days, simultaneously fostered by infected females, and then transferred to noninfected mothers. Integrated MMTV proviruses were detected in the splenic DNA of 8-week-old BM recipients by semiquantitative polymerase chain reaction (PCR) [T. V. Golovkina *et al.*, *J. Virol.* **71**, 3895 (1997)]. At that time, all KO mice were fully reconstituted with T and B cells (as determined by fluorescence-activated cell sorter analysis) and developed additional normal-size PPs (5.6 per mouse; 5, 5, 5, 5, 9, 5, 5, 6, and 5 in individual mice). Densitometry was done on the Nighthawk gel documentation system (PDI, Huntington Station, NY).
19. V. Buggiano *et al.*, *Scand. J. Immunol.* **49**, 269 (1999). An MMTV variant capable of infecting mice with H-2^b locus was used in this study.
20. H. Acha-Orbea and H. R. MacDonald, *Annu. Rev. Immunol.* **13**, 459 (1995).
21. K. Pfeffer *et al.*, *Cell* **73**, 457 (1993).
22. M. Pasparakis *et al.*, *Proc. Natl. Acad. Sci. U.S.A.* **94**, 6319 (1997).
23. D. D. Chaplin and Y. Fu, *Curr. Opin. Immunol.* **10**, 289 (1998); N. Debard, F. Sierro, J. P. Kraehenbuhl, *Semin. Immunol.* **11**, 183 (1999).
24. Y. X. Fu, G. Huang, Y. Wang, D. D. Chaplin, *J. Exp. Med.* **187**, 1009 (1998). However, our preliminary data show that lymphotoxin α involved in FDC generation is not important for B cell–dependent development of FAE.
25. Similarly, B cell–dependent FDCs influence sensitivity to prions [M. A. Klein *et al.*, *Nature* **390**, 687 (1997)].
26. S. J. Culkin, T. Rhinehart-Jones, K. L. Elkins, *J. Immunol.* **158**, 3277 (1997); H. Marcotte *et al.*, *J. Infect. Dis.* **173**, 1034 (1996); G. Matsuzaki, H. M. Vordermeier, A. Hashimoto, K. Nomoto, J. Ivanyi, *Cell. Immunol.* **194**, 178 (1999); H. M. Vordermeier, N. Venkataprasad, D. P. Harris, J. Ivanyi, *Clin. Exp. Immunol.* **106**, 312 (1996); R. H. Lin, M. J. Mamula, A. Hardin, C. A. Janeway, *J. Exp. Med.* **173**, 1433 (1991); D. V. Serreze *et al.*, *J. Exp. Med.* **184**, 2049 (1996).
27. O. T. Chan, L. G. Hannum, A. M. Haberman, M. P. Madaio, M. J. Shlomchik, *J. Exp. Med.* **189**, 1639 (1999).
28. PP generation is a multistep process in which primary "anlage" development precedes population with lymphocytes [S. Adachi, H. Yoshida, H. Kataoka, S.-I. Nishikawa, *Int. Immunol.* **9**, 507 (1997); H. Yoshida *et al.*, *Int. Immunol.* **11**, 643 (1999)]. These PP formation centers are too small to be detected using a stereomicroscope; however, the appearance of 9 ± 0.6 well-developed PPs in adult Igh-6 mice 14 days after B6 BM transfer supports the idea that the anlagen are predeveloped by a B cell–independent mechanism.
29. L. E. Malick and R. B. Wilson, *Stain Technol.* **50**, 265 (1975); J. Nation, *Stain Technnol.* **58**, 347 (1983); L. E. Malick and R. B. Wilson, in *Scanning Electron Microscopy*, O. Johari, Ed. (IIT Research Institute, Chicago, 1975), p. 256. Briefly, intestinal fragments containing PP were cleaned from mucus and fixed in 2.5% glutaraldehyde in 0.1% cacodylate buffer overnight at 4°C. Specimens were treated with alternating 1% osmium tetroxide and 1% thiocarbohydrazide (OTOTO method), dehydrated in graded series of acetone, critical point–dried, and sputter-coated to produce 15-nm gold coating. Samples were examined using a Jeol 35 scanning electron microscope at an accelerating voltage of 15 kV.

30. We thank L. Bechtold for her excellent assistance with SEM, M. Neutra for help with SEM data interpretation, and P. Cherry for secretarial assistance. Supported in part by NIH grants CA65795 (T.V.G.), DK53561 (A.C.), CA34196 (T.V.G. and A.C.), and AI43603 (M.S.); the Merck Foundation (A.C.); and Jackson Laboratory grants (A.C. and T.V.G.).

23 July 1999; accepted 25 October 1999

Use of Chemokine Receptors by Poxviruses

Alshad S. Lalani,[1,2*] Jennefer Masters,[1†] Wei Zeng,[1] John Barrett,[1] Rajeet Pannu,[2] Helen Everett,[2] Christopher W. Arendt,[3] Grant McFadden[1‡]

Chemokine receptors serve as portals of entry for certain intracellular pathogens, most notably human immunodeficiency virus (HIV). Myxoma virus is a member of the poxvirus family that induces a lethal systemic disease in rabbits, but no poxvirus receptor has ever been defined. Rodent fibroblasts (3T3) that cannot be infected with myxoma virus could be made fully permissive for myxoma virus infection by expression of any one of several human chemokine receptors, including CCR1, CCR5, and CXCR4. Conversely, infection of 3T3-CCR5 cells can be inhibited by RANTES, anti-CCR5 polyclonal antibody, or herbimycin A but not by monoclonal antibodies that block HIV-1 infection or by pertussis toxin. These findings suggest that poxviruses, like HIV, are able to use chemokine receptors to infect specific cell subtypes, notably migratory leukocytes, but that their mechanisms of receptor interactions are distinct.

Viruses can use a wide spectrum of cellular receptors for binding and entry to initiate an infectious process (*1, 2*). For example, HIV and simian immunodeficiency virus (SIV) are known to exploit a variety of members belonging to the chemokine receptor superfamily, most notably CXCR4 and CCR5, which, along with CD4, act as coreceptors to govern viral tropism [reviewed in (*3*)]. The identification of cell-surface receptors for poxvirus

References and Notes

[5] **Conversion by Peyer's Patch Lymphocytes of Human Enterocytes into M Cells that Transport Bacteria**

Sophie Kernéis; Anna Bogdanova; Jean-Pierre Kraehenbuhl; Eric Pringault

Science, New Series, Vol. 277, No. 5328. (Aug. 15, 1997), pp. 949-952.

Stable URL:

http://links.jstor.org/sici?sici=0036-8075%2819970815%293%3A277%3A5328%3C949%3ACBPPLO%3E2.0.CO%3B2-Y

[10] **A 39-kDa Protein on Activated Helper T Cells Binds CD40 and Transduces the Signal for Cognate Activation of B Cells**

Randolph J. Noelle; Meenakshi Roy; David M. Shepherd; Ivan Stamenkovic; Jeffrey A. Ledbetter; Alejandro Aruffo

Proceedings of the National Academy of Sciences of the United States of America, Vol. 89, No. 14. (Jul. 15, 1992), pp. 6550-6554.

Stable URL:

http://links.jstor.org/sici?sici=0027-8424%2819920715%2989%3A14%3C6550%3AA3POAH%3E2.0.CO%3B2-W

[22] **Peyer's Patch Organogenesis is Intact yet Formation of B Lymphocyte Follicles is Defective in Peripheral Lymphoid Organs of Mice Deficient for Tumor Necrosis Factor and its 55-kDa Receptor**

Manolis Pasparakis; Lena Alexopoulou; Matthias Grell; Klaus Pfizenmaier; Horst Bluethmann; George Kollias

Proceedings of the National Academy of Sciences of the United States of America, Vol. 94, No. 12. (Jun. 10, 1997), pp. 6319-6323.

Stable URL:

http://links.jstor.org/sici?sici=0027-8424%2819970610%2994%3A12%3C6319%3APPOIIY%3E2.0.CO%3B2-1